JOURNAL OF MATERIALS SCIENCE 27 (1992) 2490–2500

Flash calcines of kaolinite: effect of process variables on physical characteristics

R. C. T. SLADE*, T. W. DAVIES, H. ATAKÜL, R. M. HOOPER
Department of Chemistry and School of Engineering, University of Exeter, Exeter EX4 4QD, UK

D. J. JONES
Laboratoire des Agrégats Moléculaires et Matériaux Inorganiques, URA CNRS 79, Université des Sciences et Techniques du Languedoc, 34060 Montpellier Cedex, France

The physical transformation of powdered kaolinite associated with rapid dehydroxylation during flash calcination has been followed using pycnometry, thermogravimetry, electron microscopy, X-ray powder diffraction and infrared spectroscopy. 116 partially dehydroxylated kinetically-frozen calcines were produced in a laboratory flash calciner covering the following ranges of process variables: calciner temperature 700–1000 °C, rate of heating to calciner temperature 4700–15000 K s^{-1}, residence time at the calciner temperature 0.1–1.5 s, He or N_2 calciner atmosphere. From the analyses of these calcines a picture of the changes in physical characteristics caused by flash heating of kaolinite has emerged and is described.

1. Introduction

1.1. Calcination

The heat treatment (calcination) of clays and similar materials is a common industrial process with the principal objective of stabilization of the materials by dehydroxylation (removal of water). Kaolinite (china clay, $Al_2Si_2O_5(OH)_4$—sometimes written as $Al_2O_3 \cdot 2SiO_2 \cdot 2H_2O$) is a raw material of considerable industrial significance on an international scale [1]. The kaolinite structure is built by stacking lamellae composed of a pair of silica and alumina sheets. The silica sheets contain vertex-shared SiO_4 tetrahedra, while the alumina sheets contain edge-shared AlO_6 octahedra. Three of the four hydroxyl groups associated with the alumina sheets lie in the intersheet space between successive sheet pairs, while the fourth is intrasheet (between the silica and alumina sheets). Dehydroxylation is a rate process and calcines can be kinetically frozen at various stages of structural reorganization.

In industrial soak calcination, complete dehydroxylation is achieved by holding the clay at a sufficiently high temperature ($600 < T < 1100$ °C) for a sufficient length of time (~ 1 h) in an oil- or gas-fired furnace. The rate at which the clay is brought to the calcination temperature is low and is not used as a process variable; the resulting meta-kaolin has a density ~ 2.74 g cm^{-3} [2]. Overheating kaolinite results in the formation of mullite ($Al_6Si_2O_{13}$) and cristobalite (SiO_2), generally considered undesirable (as the abrasiveness of the calcine is increased). The properties of meta-kaolinite formed by soak calcination are a useful benchmark against which the properties of flash calcines (see below) can be compared. There have been many laboratory studies of physical and chemical transformation of kaolinite under such soak calcination conditions, probing both structural changes [3–8] and also the kinetics of dehydroxylation [9–11].

The present laboratory-based study concerns the physical characteristics of flash calcines of kaolinite, and in particular their variations with carefully controlled process variables (see below). The specific data presented are densities, degrees of dehydroxylation, transmission electron micrographs (TEM), infrared spectra and X-ray powder diffraction patterns.

1.2. Flash calcination

If kaolinite particles are heated at such a speed that the steam released within them is generated faster than it can escape by diffusion, structural disruption is likely. Such structural disruption may endow the resulting calcine with desirable or interesting properties, such as internal voids [12]. The diameters of such voids are approximately equal to the wavelengths for visible light, producing light scattering and imparting opacity to the material (then usable as an effective paper covering). Construction in our laboratory of a furnace to allow kaolinite particles to be subjected to thermal histories comparable to those in industrial flash calciners has been described elsewhere [13].

In industrial flash calcination, cold powdered clay is passed through a gas or oil flame and then quenched by injection of cold air. The laboratory simulation of this process involves plunging a stream of clay particles into a co-flowing stream of hot He(g) or N_2(g)

---

* Author to whom correspondence should be addressed.

0022-2461

(which is in downward laminar flow) in a vertical electrically-heated reaction tube. Flash calcines produced in this way have quite different properties from corresponding soak calcines [12, 14–16]. In particular, the short residence times in the calciner lead to calcines that are incompletely dehydroxylated and that can have densities lower than those of soak calcines (this being consequential on the voids present in flash calcines).

A picture of structural changes during flash calcination is being developed using high resolution magic-angle-spinning ^{27}Al and ^{29}Si nuclear magnetic resonance (MAS–NMR) techniques [17, 18]. The derived composite picture of flash calcination is that of a material transforming increasingly completely from kaolinite to a single product. Once formed, the product appears to undergo little further chemical reaction during its short time in the calciner. Prolonged (soak) thermal treatment of flash calcines produces materials comparable (e.g. densities) to those from soak calcination. The transformations towards those products are much slower than the initial step giving the flash calcine.

Previous studies of flash calcination of kaolinite have involved a limited range of calcination process variables [12–18]. In the present study, process variables such as calciner temperature, T, heating rate, Δ, from cold to the calciner temperature, residence time in the calciner (τ, s) and calciner atmosphere (flowing dry He(g) or N_2(g)) have been systematically varied in order to investigate consequential variations in the physical properties of the resulting calcines.

2. Experimental procedure

The kaolinite feedstock was commercial grade SPS clay (English China Clays International, St. Austell, Cornwall). Ninety per cent of the powder was $< 2\ \mu$m particle size. X-ray analysis gave SiO_2 46.2%, Al_2O_3 38.7%, Fe_2O_3 0.56%, TiO_2 0.09%, CaO 0.20%, MgO 0.20%, K_2O 1.01%, Na_2O 0.07% and the loss on ignition (H_2O content) was 13.14%.

Flash calcination was carried out in a laminar flow furnace described elsewhere [13]. A stream of kaolinite particles in flowing He(g) or N_2(g) was heated from room temperature to a calciner temperature, T, by a computer-controlled heating system. Calcined material collected in a water-cooled collector probe was quenched with room, temperature N_2(g). Residence time, τ, for the particles in the isothermal reaction zone at a given T was set by controlling the gas flow rate and the position of the collector probe. Heating rate, Δ, was calculated from the gas flow rate and the temperature difference that solid particles experienced in the heating zone between the entrance of the furnace and isothermal reaction zone [14]. The design and conditions of the furnace are such that laminar flow is always established in the furnace. Analysis of the heat transfer process to and within particles and their terminal velocity shows that the particles effectively follow the transport gas temperature and achieve the set calciner temperature, T, in a few milliseconds [12].

116 different flash calcines were prepared using differing combinations of process variables in the ranges $0.1 \leqslant \tau < 1.5$ s, $700 \leqslant T \leqslant 1200\,^{\circ}$C, $4700 \leqslant \Delta \leqslant 15000$ K s^{-1} and flowing He(g) or N_2(g).

Densities ρ (g cm^{-3}) were measured by pycnometry with replacement of water. The density of kaolinite measured in water and various organic liquids shows no significant differences [19]. Densities presented are mean values (standard deviation $< 2\%$). Degrees of dehydroxylation (α, %) were determined by thermogravimetry using a Stanton TG 750 instrument (flowing N_2(g)); mean values are presented. Transmission electron microscopy (TEM) employed a Philips EM300 microscope. X-ray powder diffraction patterns (Ni filtered CuK_α radiation) were recorded using a computer-controlled Philips PW1050 goniometer incorporating accumulation of multiple scans. Infrared spectra (KBr discs, 1 mg sample: 500 mg KBr) were recorded in the range 400–4000 cm^{-1} (Perkin–Elmer 398 instrument).

3. Results

3.1. Densities and dehydroxylation

Variations of calcine density, ρ, with residence time, τ, are shown in Fig. 1 for calciner temperature, $T = 1000\,^{\circ}$C, and at heating rates, $\Delta = 4700$ and 8000 K s^{-1}, in He(g) and N_2(g). Scatter evident in the data is a measure of the controllability of process

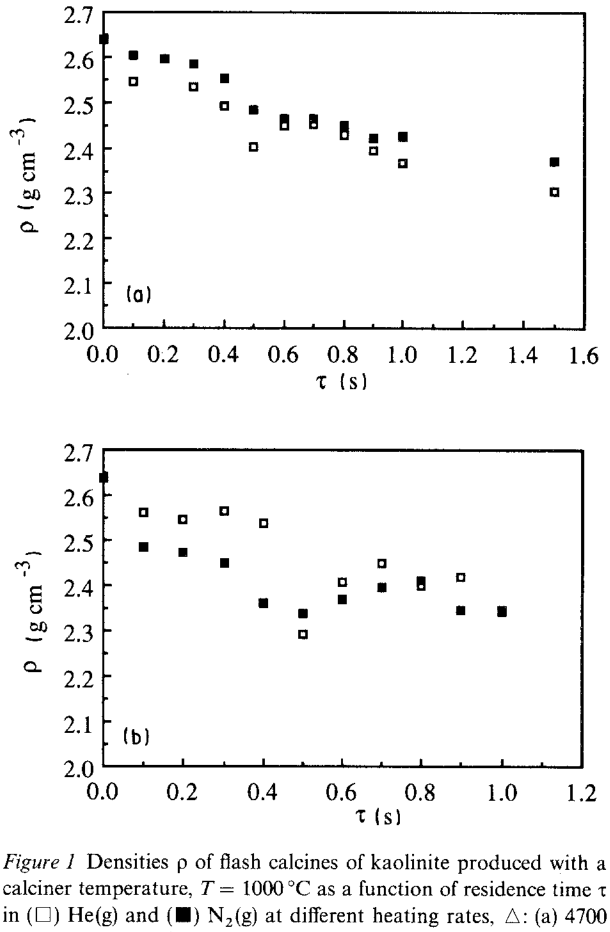

Figure 1 Densities ρ of flash calcines of kaolinite produced with a calciner temperature, $T = 1000\,^{\circ}$C as a function of residence time τ in (□) He(g) and (■) N_2(g) at different heating rates, Δ: (a) 4700 and (b) 8000 K s^{-1}.

variables. At 4700 K s^{-1} progressive decreases in ρ with increasing τ are evident. At 8000 K s^{-1}, however, minima in ρ occur at τ ≈ 0.5 s with ρ then being lower than those obtained for any calcine at 4700 K s^{-1}. A similar minimum has been reported previously [16].

Variations in ρ with heating rate and T at a fixed $\tau = 0.5$ s are shown in Fig. 2 for He(g) and N_2(g). Increases in heating rate and T are both seen to lead to decreases in ρ. The steepest decreases in ρ with increasing T occur at the highest heating rates.

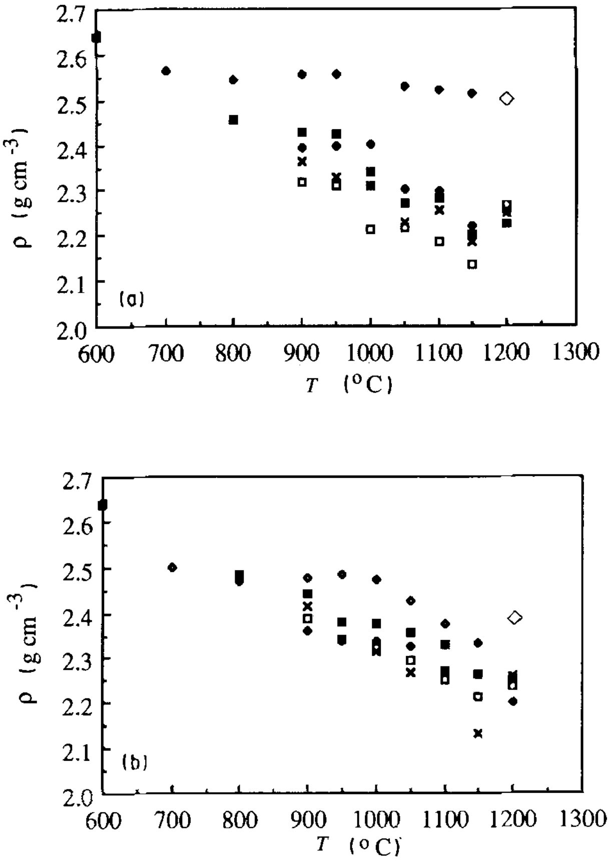

Figure 2 Densities ρ of flash calcines of kaolinite produced at a range of calciner temperatures, T, with a fixed residence time $\tau = 0.5$ s as a function of heating rate Δ: (a) in He(g), (b) in N_2(g): (◇) 4700; (◆) 8000; (■) 10000; (□) 12000 and (×) 15000.

Typical transmission electronmicrographs are shown in Fig. 3. Although not susceptible to quantitative analysis, these pictures show extensive bubble-like areas (voids) within calcine particles, as reported previously [12]. Raw kaolinite is free of such bubbles, which are caused by structural disruption during fast heating (see above).

Fig. 4 presents the variation of flash calcine density, ρ, with degree of dehydroxylation, α, in He(g) and N_2(g). Straight lines shown are those arising from the (simplistic) assumption that particle volumes remain constant during dehydroxylation (while particle masses change) [12]. ρ is typically lower than that prediction. This fact and the known increase in density during soak calcination (without voidage) indicates increases in particle volumes during flash calcination, a major part of which will be due to void formation. The scatter evident in the plots is a consequence of presentation of data on calcines produced with a wide range of process conditions. Lower densities tend to be associated with higher degrees of dehydroxylation.

3.2. X-ray patterns

Fig. 5 shows the variation with residence time τ of the X-ray powder diffraction pattern for calcines produced with $T = 1000$ °C and $\Delta = 4700$ K s^{-1} in He(g). Calcines produced under these conditions have the most gradual change in X-ray diffraction pattern with increasing τ. At $\tau = 0.1$ s the dominant feature is the pattern of as-yet untransformed kaolinite, but the amorphous background due to transformed material is evident at low intensity. As τ is increased, the kaolinite pattern dwindles and the pattern of transformed material becomes predominant.

Fig. 6 shows the corresponding variation using N_2(g). The change of pattern with increasing τ is very similar to that with He(g), all other variables being the same. Examination of Fig. 1 shows similar trends in variation of ρ with τ in the two cases. Very similar calcines appear to be produced in the different dry atmospheres.

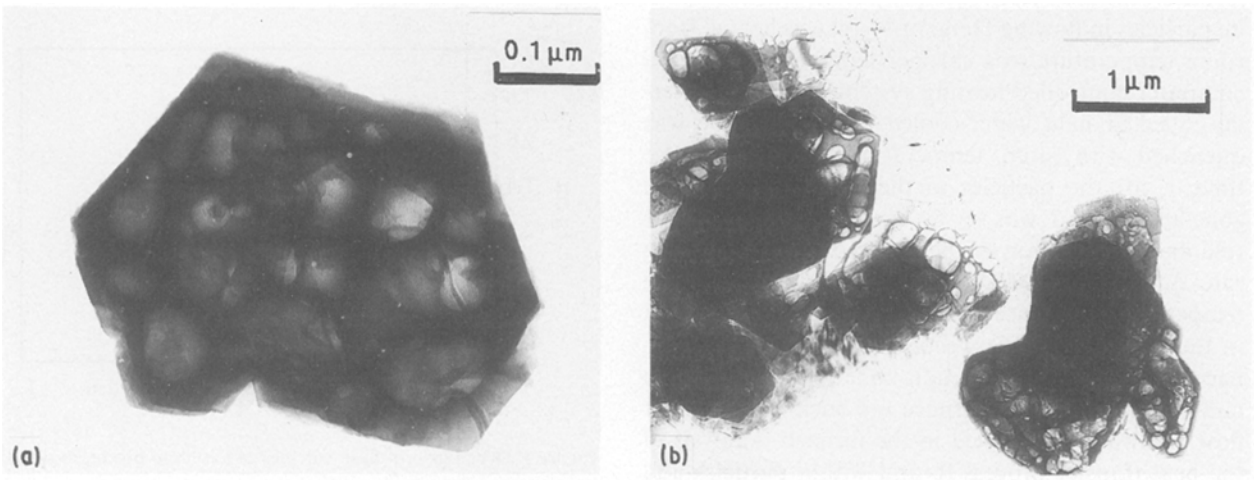

Figure 3 Transmission electronmicrographs of a flash calcine of kaolinite produced in He(g) with calciner temperature, $T_r = 1000$ °C, heating rate, $\Delta = 8000$ K s^{-1} and residence time, $\tau = 0.5$ s. Scale markers are shown.

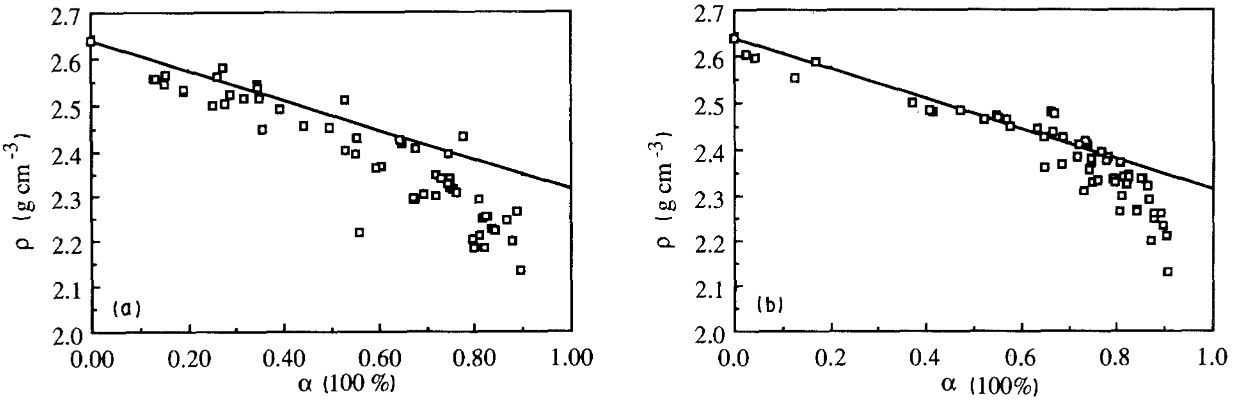

Figure 4 Variation of density ρ of flash calcines of kaolinite with degree of dehydroxylation α: (a) in He(g) and (b) in N_2(g).

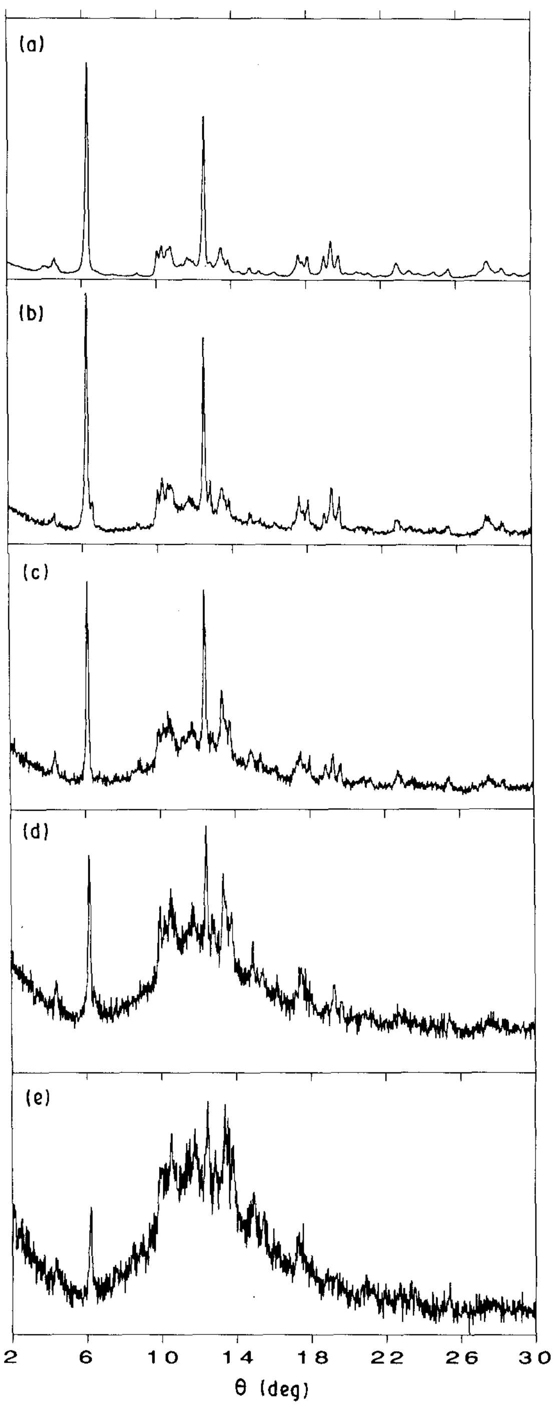

Figure 5 X-ray powder diffraction patterns of kaolinite and of flash calcines (calciner temperature, $T = 1000\,^{\circ}C$, heating rate, $\Delta = 4700\ K\ s^{-1}$; He(g)) with increasing calciner residence times τ: (a) kaolinite; (b) 0.1; (c) 0.5; (d) 1.0 and (e) 1.5 s.

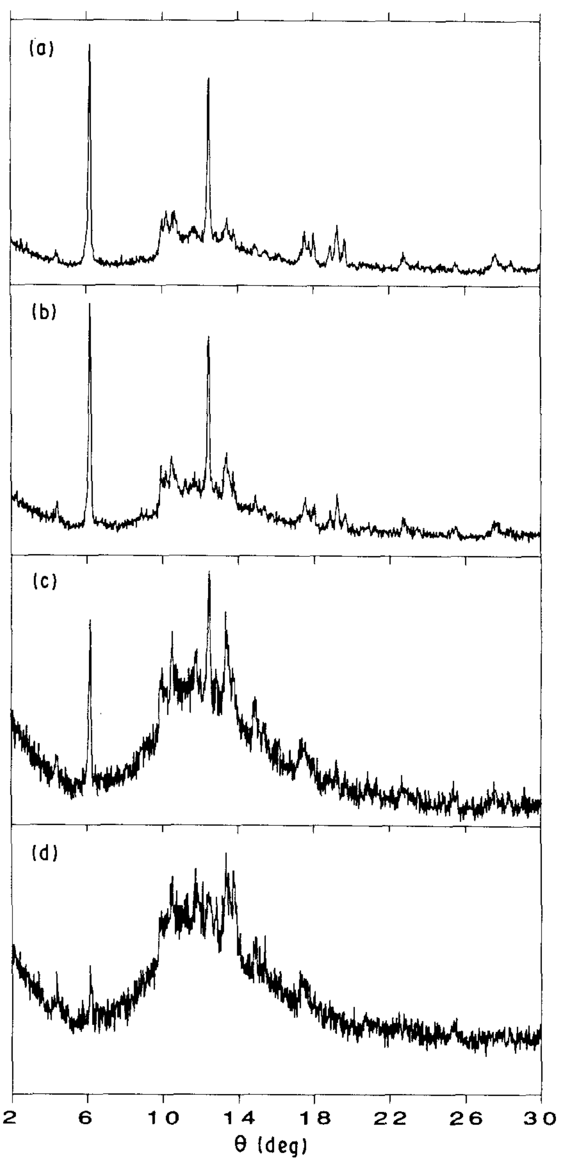

Figure 6 X-ray powder diffraction patterns of flash calcines of kaolinite (calciner temperature, $T = 1000\,^{\circ}C$, heating rate, $\Delta = 4700\ K\ s^{-1}$; N_2(g)) with increasing calciner residence times τ: (a) 0.1; (b) 0.5; (c) 1.0 and (d) 1.5 s.

Fig. 7 shows the variation with calciner temperature, T, of the X-ray powder diffraction patterns for calcines produced with $\Delta = 4700\ K\ s^{-1}$ and $\tau = 0.5$ s in He(g). The patterns are all very similar in form. Examination of Fig. 2 indicates that, under these conditions, calcine density varies little with T, but at

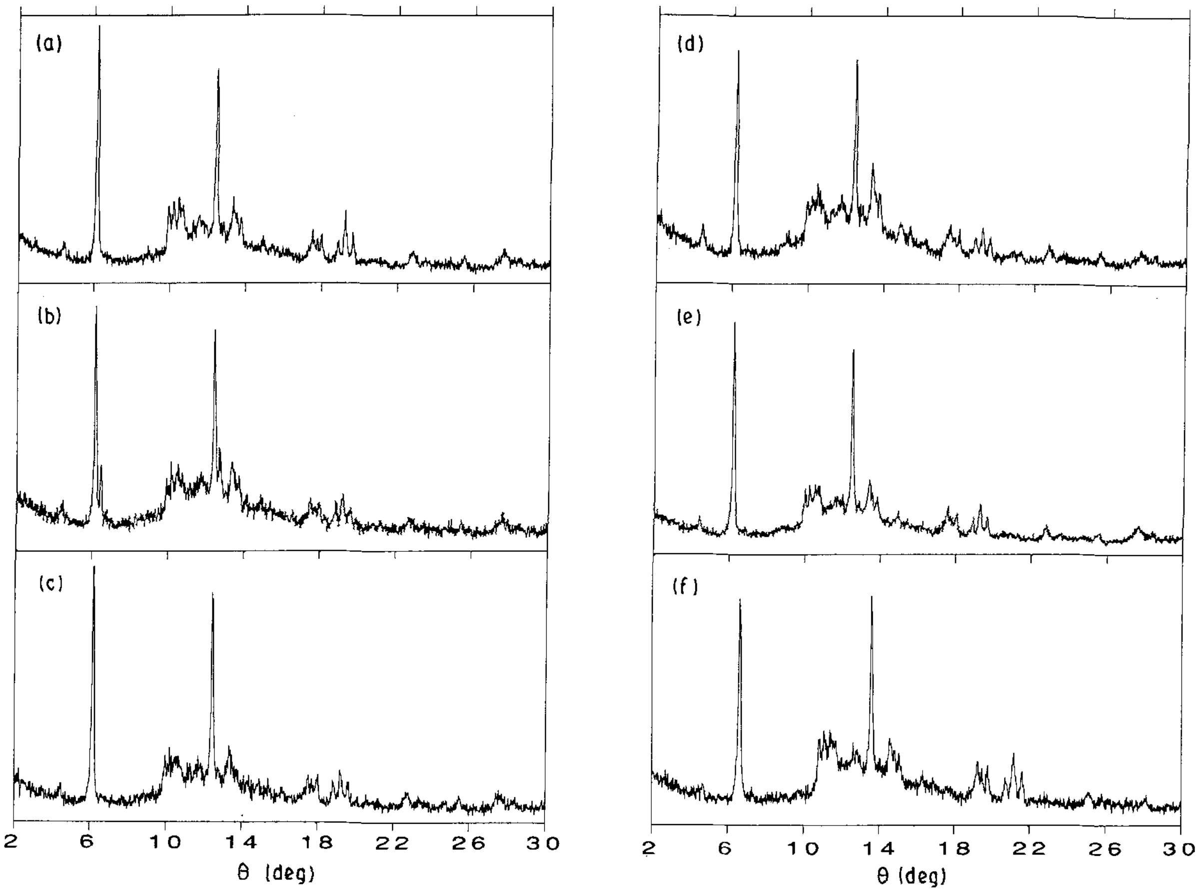

Figure 7 X-ray powder diffraction patterns of flash calcines of kaolinite (calciner residence time, $\tau = 0.5$ s, heating rate, $\Delta = 4700$ K s^{-1}; He(g)) as a function of calciner temperature, T: (a) 700; (b) 800; (c) 900; (d) 1000; (e) 1100 and (f) 1200°C.

higher Δ the density of the resulting calcine does decrease as T is increased.

Fig. 8 shows the variation with heating rate, Δ, of the X-ray powder diffraction patterns for calcines produced with $T = 1000$°C and $\tau = 0.5$ s in He(g). It is very clear from this, and also from Fig. 2, that heating rate has a profound influence on the nature of the calcine produced at fixed T and τ. Density decreases with increasing Δ as voidage is increased. The diffraction patterns indicate that calcination is more complete at higher Δ; this is also evident in the increasing degrees of dehydroxylation at the decreased densities (see Figs 2 and 4) obtained at higher Δ.

There was no evidence in the X-ray powder pattern of any flash calcine produced in this work for the formation of any crystalline mullite or cristobalite. This contrasts with the case of soak calcines produced at ca. 1000 °C [7]. Further transformation of flash calcines towards materials similar to soak calcines is very much slower than the initial transformation in the flash calciner.

3.3. Infrared spectra

Strong bands for kaolinite are known to occur at 3700, 3621, 1100, 1032, 1008, 913, 694, 539, 471 and 431 cm^{-1} [20–23]. The high frequency bands arise from stretching of the intersheet hydroxyl group (3700 cm^{-1}) and of the intrasheet hydroxyl group (3621 cm^{-1}), this doublet being used for semi-quantitative estimation of kaolinite content of minerals

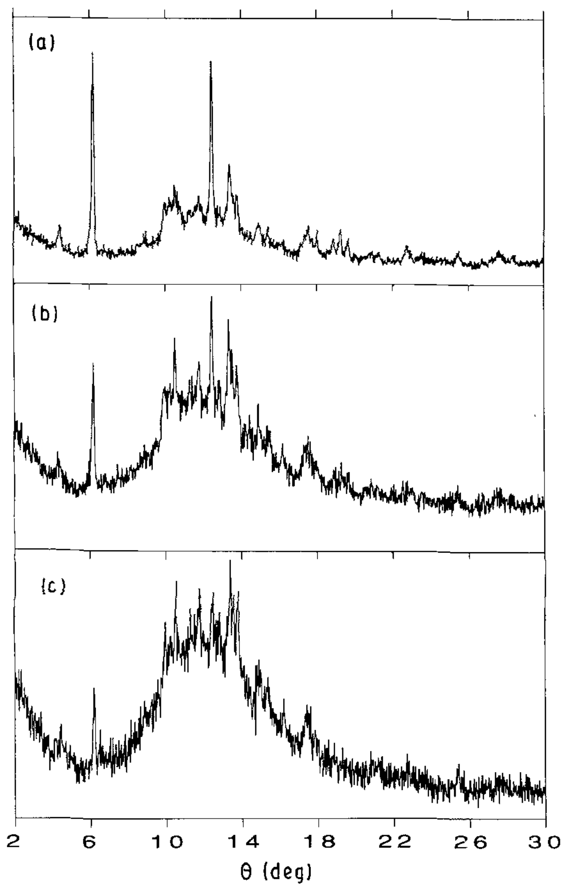

Figure 8 X-ray powder diffraction patterns of flash calcines of kaolinite (calciner temperature, $T = 1000$ °C, calciner residence time, $\tau = 0.5$ s, He(g)) as a function of heating rate, Δ: (a) 4700; (b) 8000 and (c) 15000 K s^{-1}.

TABLE 1 Assignment of infrared bands of kaolinite and meta-kaolinite [26]

	Si–O bond (tetrahedral Si)	AlO–H bond (octahedral Al)	Al–O bond (octahedral Al)
Kaolinite	1114 ms 1096 m, (sh) 1072 s, br 1060 s, sh 1035 s 1012 s 794 m 752 m 693 m 471 s 430 mw, sh 411 mw 370 mw 345 ms	938 m, (sh) 914 ms 789 m, (sh)	540 s 370 mw 345 ms
Meta-kaolinite (fully dehydroxylated, soak calcine)	1260 w, sh 1203 s, sh 1152 s, sh 1071 s, br 665 w, sh 479 m 456 m, br 428 m, sh	807 m, br	554 w, sh

s = strong, m = medium, w = weak, br = broad, sh = shoulder, (sh) = shoulder in some spectra

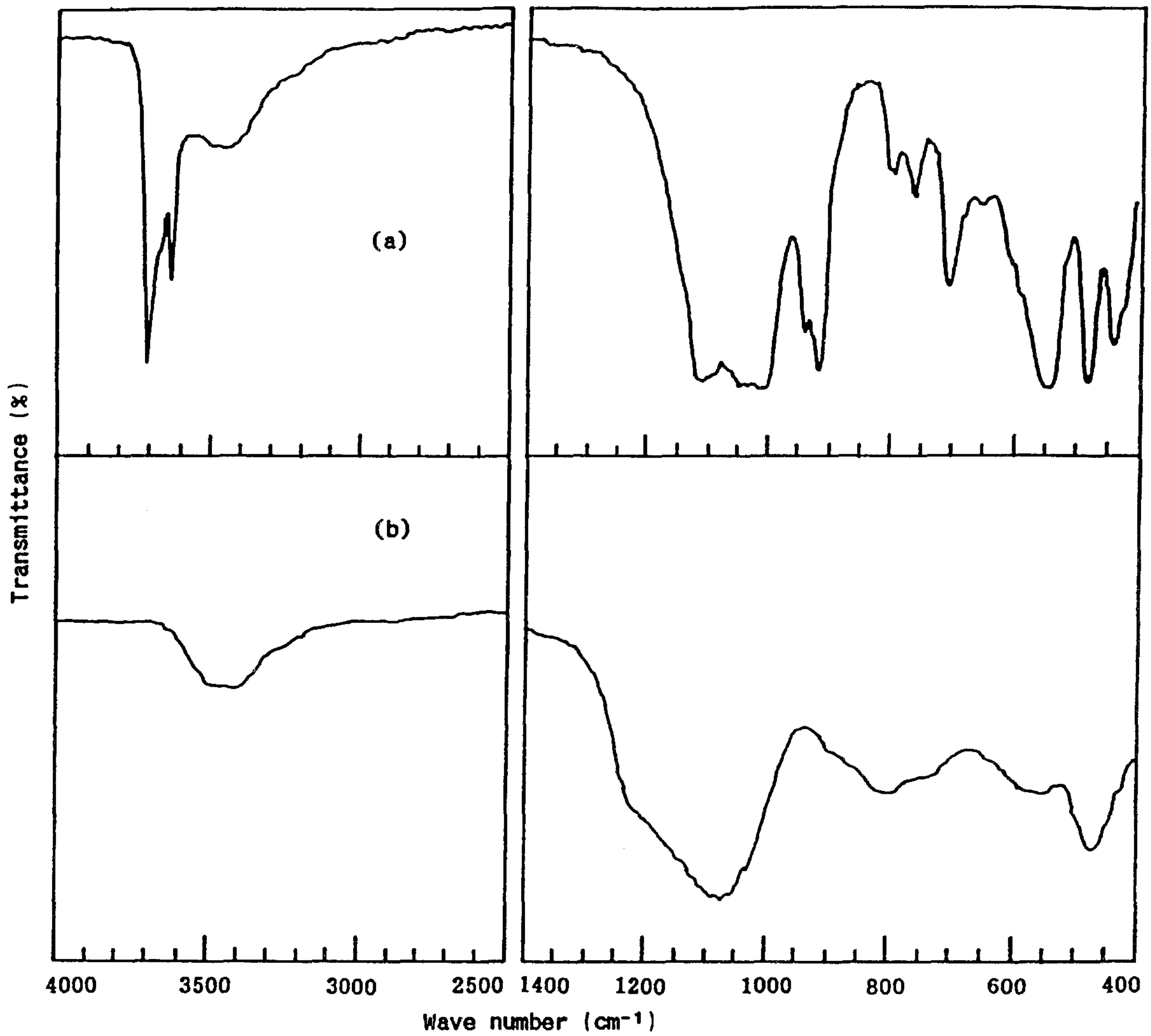

Figure 9 Infrared spectra of (a) kaolinite and (b) a soak calcine produced at 1000 °C.

[23, 24]. The 1100–1000 cm^{-1} region is known as the silicate region, while 1000–400 cm^{-1} is the aluminosilicate region. Al–O–H deformation bands at 938 and 916 cm^{-1} arise from intersheet and intrasheet hydroxyls and are characteristic of kaolinite [25]. Table I gives assignments of the infrared bands at < 1400 cm^{-1} for kaolinite and meta-kaolinite (from soak calcination) following Percival *et al.* [26].

Fig. 9 shows the infrared spectrum characteristic of the raw kaolinite used in this work and also that of a derived soak calcine (soaked in air at 1000 °C for 5 h), the latter being a totally dehydroxylated material. The region 2500–1400 cm^{-1} is omitted, containing no representative bands of interest.

Fig. 10 shows the infrared spectra of calcines produced at $T = 1000$ °C and $\Delta = 4700$ K s^{-1} as a function of calciner residence time τ in He(g). In calcines produced at 1000 °C, this series has the most gradual decrease in density (see earlier) and the most gradual change in the infrared spectra. The spectra show the progressive dehydroxylation with increasing τ, e.g. the decreasing intensities in the doublet at 3700 and 3621 cm^{-1} arising from hydroxyl stretching. The spectra are consistent with NMR studies [18] of flash calcination of kaolinite, which indicated progressive transformation of kaolinite to a single product. The progressive disappearance of the doublet corresponds to a decreasing content of residual untransformed

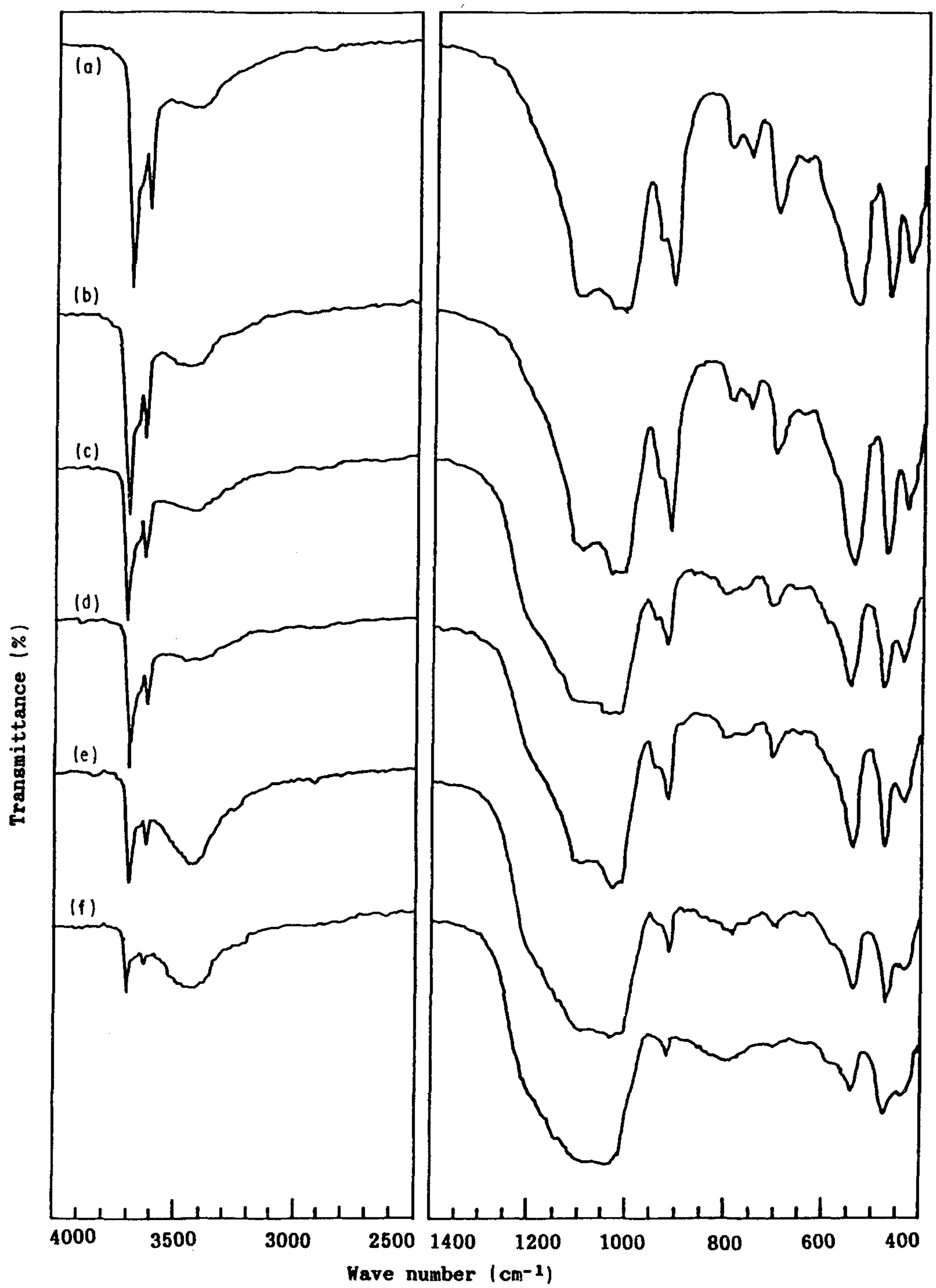

Figure 10 Infrared spectra of flash calcines of kaolinite (calciner temperature, $T = 1000$ °C, heating rate, $\Delta = 4700$ K s^{-1}; He(g)) as a function of calciner residence time τ: (a) 0.1; (b) 0.3; (c) 0.5; (d) 0.7; (e) 1.0 and (f) 1.5 s.

kaolinite and of kaolinite-like regions in the calcine. It would be too simplistic to assume that the (transformed) product is necessarily fully dehydroxylated (it would then follow that the degree of dehydroxylation allows quantification of residual kaolinite); ^{1}H NMR studies of soak calcination having revealed a step-wise dehydroxylation in soak calcination [27] and it has been suggested previously that regions of kaolinite-like structure persist in calcines [18, 28, 29]. Transformed material is known [6, 18] to contain a disordered aluminosilicate network with Si and Al in a range of regular and distorted geometries, this leading to the loss of structure in the spectral silicate and aluminosilicate regions.

Fig. 11 shows the infrared spectra of calcines produced with a fixed calciner residence time $\tau = 0.5$ s and a low heating rate $\Delta = 4700$ K s^{-1} as a function of calciner temperature, T, in He(g). In this series of calcines α varies from 16% ($T = 700$ °C) to 30% ($T = 1200$ °C), but the infrared spectra are all very similar (dominated by untransformed material). Fig. 12 shows spectra for calcines produced using the same residence time and gas, but now with the highest heating rate employed ($\Delta = 15000$ K s^{-1}). In this series of calcines α varies from 59% ($T = 900$ °C) to 87% ($T = 1200$ °C). Comparison of Figs 11 and 12 (and also of the degrees of dehydroxylation in the two cases) again illustrates that heating rate is a highly

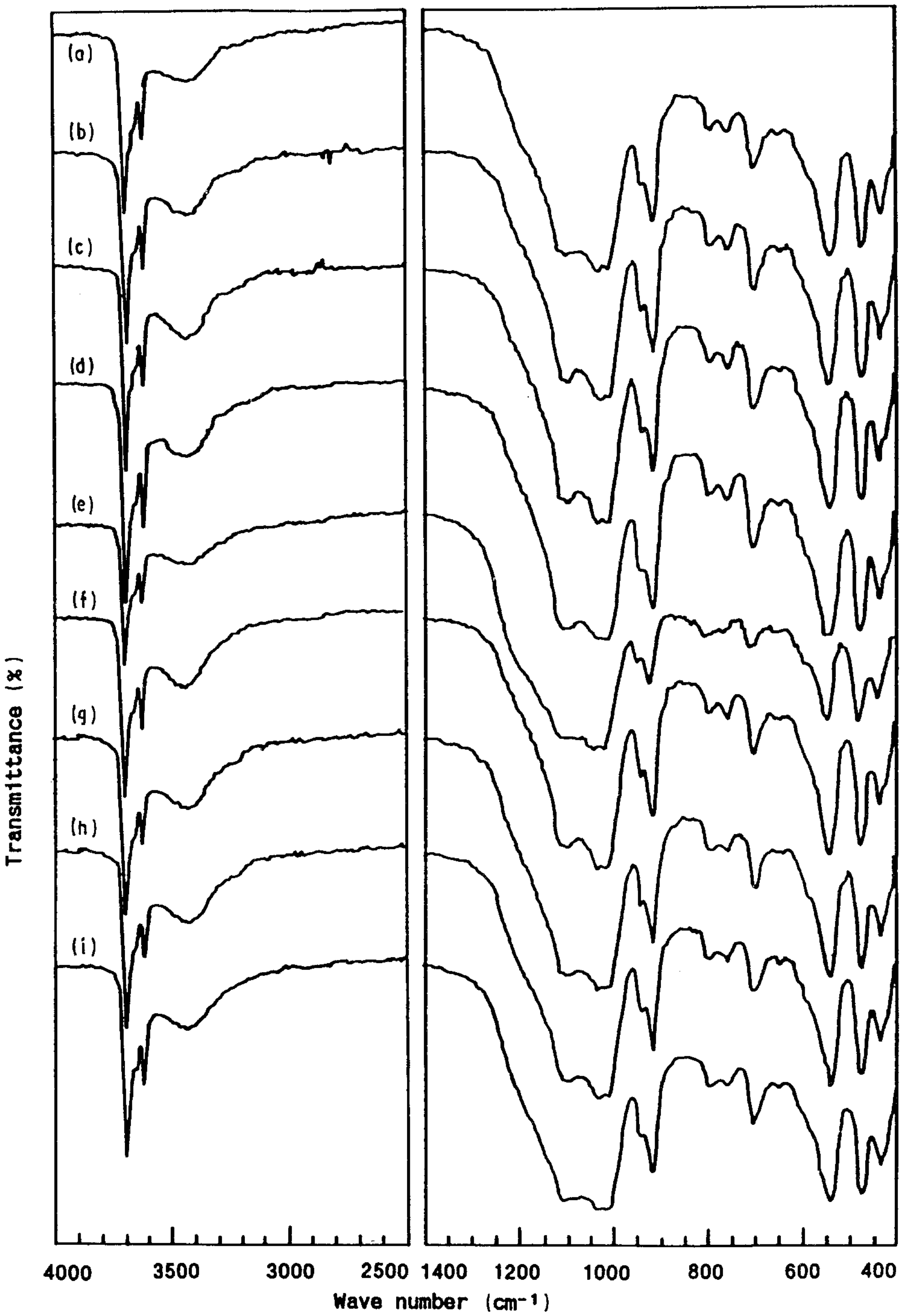

Figure 11 Infrared spectra of flash calcines of kaolinite (calciner residence time, $\tau = 0.5$ s, heating rate, $\Delta = 4700$ K s^{-1}; He(g)) as a function of calciner temperature, T: (a) 700; (b) 800; (c) 900; (d) 950; (e) 1000; (f) 1050; (9) 1100; (h) 1150 and (i) 1200 °C.

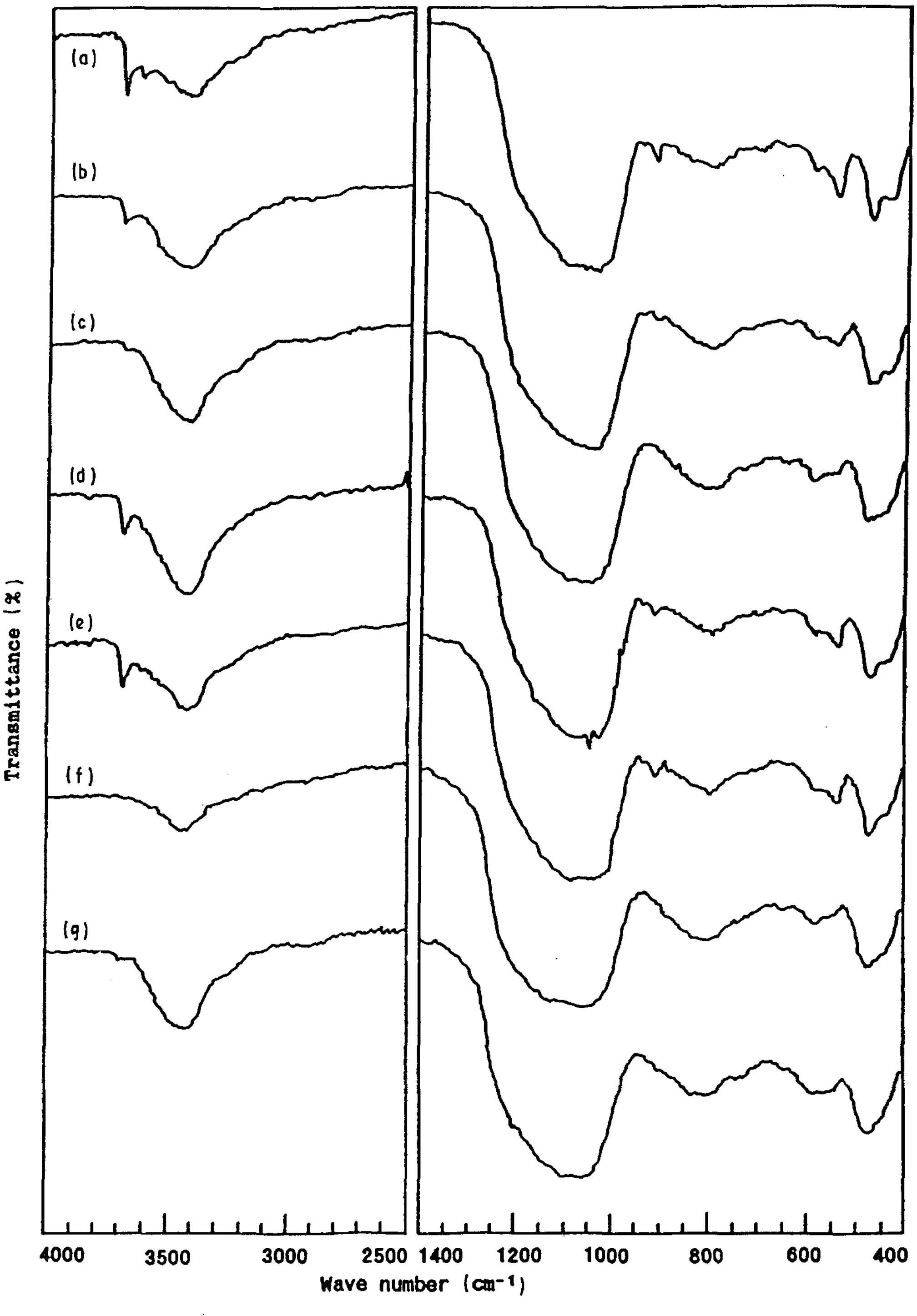

Figure 12 Infrared spectra of flash calcines of kaolinite (calciner residence time, $\tau = 0.5$ s, heating rate, $\Delta = 15000$ K s^{-1}; He(g)) as a function of calciner temperature, T: (a) 900; (b) 950; (c) 1000; (d) 1050; (e) 1100; (f) 1150 and (g) 1200 °C.

significant variable in flash calcination—higher heating rates leading to greater dehydroxylation (more complete transformation to product, as evident from X-ray patterns above) if all other process variables are held constant.

The spectra of raw kaolinite ($\alpha = 0\%$ by definition), a soak calcine ($\alpha = 100\%$, see above) and a flash calcine ($T = 1000$ °C, $\tau = 0.5$ s, $\Delta = 4700$ K s^{-1}, $\alpha = 76\%$) are compared in Fig. 13. The contribution to the spectrum of the flash calcine arising from transformed material (the total spectrum is a superposition of this and that for residual untransformed kaolinite) is similar to that for the soak calcine (predominantly meta-kaolinite). This is a consequence of both materials having massively disordered aluminosilicate networks. However, the materials are known to be different; the ^{27}Al NMR spectra of soak calcines exhibit a peak assigned to some Al in near-regular penta-coordination [8, 28, 29], while those of flash calcines do not [18]. Infrared spectra are unlikely to provide insight into the differences between soak and flash calcines.

4. Concluding discussion

116 differently produced flash calcines of kaolinite have been studied in order to assess the role of the

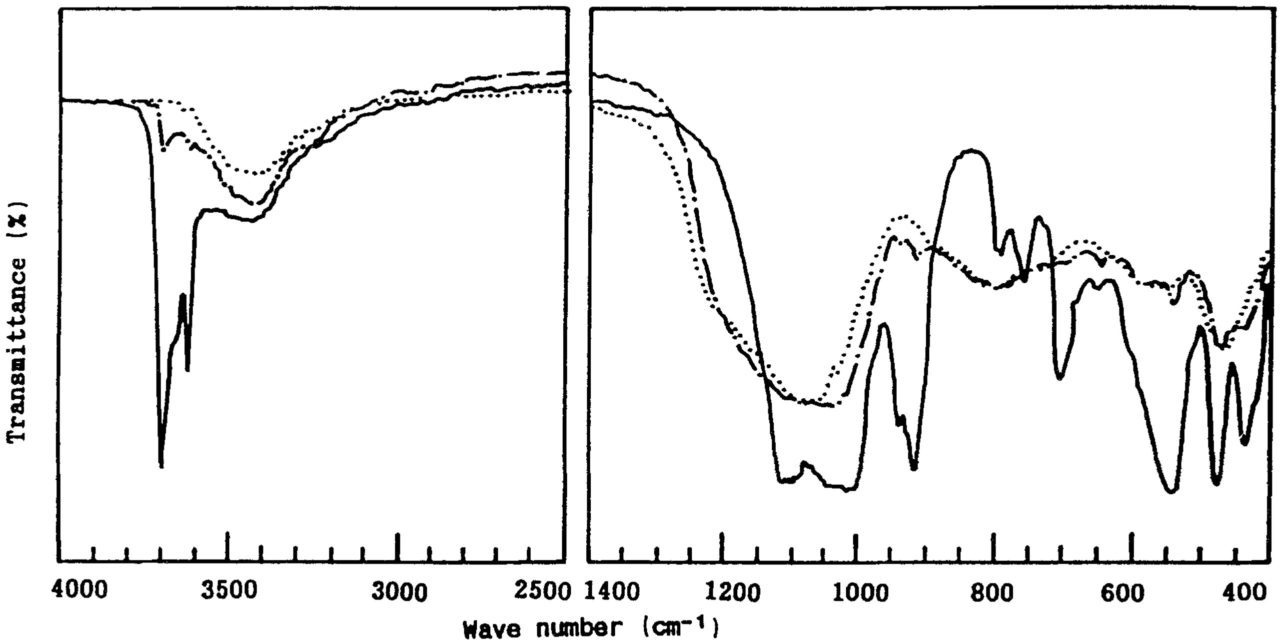

Figure 13 Comparison of the infrared spectra of: (——) kaolinite, (·····) a soak calcine produced at 1000 °C and (—·—·) a flash calcine ($T = 1000$ °C, $\tau = 0.5$ s, $\Delta = 4700$ K s^{-1}, $\alpha = 76\%$).

various process variables in determining the characteristics of the product calcine. Process variables explored were calciner temperature, heating rate (to calciner temperature), residence time (in the calciner) and calciner atmosphere.

The effect of variation of calciner atmosphere between He(g) and N_2(g) is not great (Figs 1, 5 and 6).

For a fixed initial heating rate and calciner temperature, lower densities are obtained at longer residence times due to more complete transformation of the starting material. At high heating rates a minimum in calcine density may occur at $\tau \approx 0.6$ s (Fig. 1b and Reference 16), possibly indicative of some shrinkage of greater voidage induced at the highest heating rates.

Both initial heating rate and calciner temperature have profound effects on the product, increasing either variable leading to lower density calcines (Fig.2). The lowest density calcines are those which are the most dehydroxylated (Fig. 4). An attempt to explain these gross effects of flash calcination in terms of the heat and mass transfer phenomena which occur during the transient heating of a reactive particle has been made [30]; the resulting mathematical model was used to demonstrate the sensitivity of the dehydroxylation process to surface heat transfer events.

Variations in X-ray powder diffraction patterns and infrared spectra of the calcines can be linked simply to variations in density (and hence to degree of dehydroxylation *via* Fig. 4).

The flash calcines all differ markedly from soak calcines, e.g. in having densities lower than kaolinite (soak calcines are denser than kaolinite) and in the absence of any crystalline mullite or cristobalite. NMR studies indicate differences in the aluminosilicate structure of flash and soak calcines [18]; the differences in physical properties (e.g. density) do not arise only from the presence of voids in flash calcines (Fig. 3).

Acknowledgements

We thank the Science and Engineering Research Council for supporting this study under grant GR/E 81999. H. A. thanks Istanbul Technical University for study leave.

References

1. W. D. KELLER, *Geology Today* (1985) 109.
2. R. E. GRIM, in "Clay Mineralogy" 2nd Edn (McGraw-Hill, New York, 1968).
3. G. W. BRINDLEY and M. NAKAHIRA, *Nature*, **181** (1958) 1333.
4. *Idem*, *J. Amer. Ceram. Soc.* **42** (1959) 319.
5. A. K. CHAKRABORTY and D. K. GHOSH, *ibid.* **61** (1978) 170.
6. R. H. MEINHOLD, K. J. D. MACKENZIE and M. E. BOWDEN, *ibid.* **68** (1985) 293.
7. I. W. M. BROWN, K. J. D. MACKENZIE and I. W. M. BROWN, *J. Mater. Sci. Lett.* **4** (1985) 163.
8. J. F. LAMBERT, W. S. MILLMAN and J.J. FRIPIAT, *J. Amer. Chem. Soc.* **111** (1989) 3517.
9. F. TOUSSAINT, J. J. FRIPIAT and M. C. GASTUCHE, *J. Phys. Chem.* **67** (1963) 26.
10. G. W. BRINDLEY, J. H. SHARP, J. H. PATTERSON and M. NAKAHIRA, *The Amer. Mineral.* **52** (1967) 201.
11. J.M. CRIADO, A. ORTEGA, C. REAL and E. T. TORRES, *Clay Miner.* **19** (1984) 653.
12. D. BRIDSON, T. W. DAVIES and D. P. HARRISON, *Clays and Clay Miner.* **33** (1985) 258.
13. T. W. DAVIES, *High Temp. Technol.* **2** (1984) 141.
14. *Idem*, *Chem. Eng. Res. Des.* **63** (1985) 82.
15. T. W. DAVIES and R. M. HOOPER, *J. Mater. Sci. Lett.* **4** (1985) 39.
16. T. W. DAVIES, *ibid.* **5** (1986) 186.
17. R. C. T. SLADE and T. W. DAVIES, *Colloids and Surf.* **36** (1989) 119.
18. *Idem*, *J. Mater. Chem.* **1** (1991) 361.
19. S. I. WADA and K. WADA, *Clay and Clay Miner.* **12** (1977) 289.
20. B. D. SAKSENA, *Trans. Faraday Soc.* **57** (1961) 242.
21. J. G. MILLER, *J. Phys. Chem.* **65** (1961) 800.
22. P. TARTE, *Spectrochimica Acta*, **23A** (1967) 2127.

23. H. W. van den MAREL and H. BEUTELSPACHER, in "Atlas of Infrared Spectroscopy of Clay Minerals and Their Admixtures" (Elsevier, Amsterdam, 1976).
24. J. D. RUSSELL, in "A Handbook of Determinative Methods in Clay Mineralogy", edited by M. J. Wilson (Blackie, New York, 1987) p.133.
25. J. A. RAUSELL-COLOM and J. M. SERRATOSA, in "Chemistry of Clays and Clay Minerals", edited by A. C. D. Newman (Minerological Society, London, 1987) p. 371.
26. H. J. PERCIVAL, J. F. DUNCAN and P. K. FOSTER, *J. Amer. Ceram. Soc.* **57** (1974) 57.
27. C. OTERO-AREAN, M. LETELLIER, B. C. GERSTEIN and J. J. FRIPIAT, in 'Proceedings of the International Clay Conference 1981–Bologna', edited by Van Olphen and Veniale (Elsevier, Amsterdam, 1982) p.73.
28. J. SANZ, A. MADANI, J. M. SERRATOSA, J. S. MOYA and S. AZA, *J. Amer. Ceram. Soc.* **71** (1988) c 418.
29. J. ROCHA and J. KLINOWSKI, *Phys. Chem. Miner.* **17** (1990) 179.
30. T. W. DAVIES and A. D. DIAPER, in Proceedings of the 2nd UK Conference on Heat Transfer–Glasgow, Vol. 2 (Institution of Mechanical Engineers, London, 1988) p. 1201.

Received 21 February
and accepted 1 May 1991